Full-color and less-speckled modified Gerchberg–Saxton algorithm computer-generated hologram floating in a dual-parabolic projection system

Chien-Yu Chen (陳建宇)[1,*], Hsuan-Ting Chang (張軒庭)[2], Tsung-Jan Chang (張琮然)[3], and Chih-Hao Chuang (莊智皓)[3]

[1]*Graduate Institute of Color and Illumination Technology, National Taiwan University of Science and Technology, Taipei 10607, China*

[2]*Department of Electrical Engineering, National Yunlin University of Science and Technology, Yunlin 64002, China*

[3]*Department of Electronics Engineering, National Yunlin University of Science and Technology, Yunlin 64002, China*

**Corresponding author: chencyue@mail.ntust.edu.tw*

Received May 17, 2015; accepted August 28, 2015; posted online October 9, 2015

This Letter proposes to apply full-color computer-generated holograms to the virtual image projection system so that the viewers can comfortably view floating images. Regarding the spatial division and distribution operation, a modified Gerchberg–Saxton algorithm is used for acquiring the phase infographics, which are input into the spatial light modulator for the reconstructed projection. Such a virtual image projection system could reach the vertical angle of view of 15°–75° and the horizontal angle of view 360°, and the mixed-light modulating proportion contains a 3 mW red light laser, a 2 mW green light laser, and a 2.6 mW blue light laser to achieve the full-color mixed-light proportion with a speckle contrast of 6.65%. The relative diffraction efficiency and root mean square error of the reconstructed image are 95.3% and 0.0524, respectively.

OCIS codes: 090.1760, 090.0090, 090.2870.

doi: 10.3788/COL201513.110901.

The computer-generated hologram (CGH) is a technology based on holographic theories[1] that simulates the interference of an object beam and a reference beam to generate holograms. Currently, a spatial light modulator (SLM) is mostly utilized for image reconstruction[2]. A CGH could record and reconstruct three-dimensional (3D) images[3–5], as well as reduce optical deviation in the optical recording process of traditional holograms[6]. The 3D phase information of an object needs to be calculated, and at least three times the operand is required for the full-color effect. Current CGHs mostly present images with monochromatic light. Nonetheless, full-color holographic displays would be a key development in 3D display technology in order to enhance the reality of the images.

A full-color holographic system has currently been completed with LEDs[7]. However, in terms of color performance and efficiency consumption, laser light presents better color purity, with better sharpness and colorfulness than LEDs do. Additionally, a laser produces high-directivity, coherent light that would not consume energy when propagating in the air and could transmit light over a distance. Accordingly, a full-color mixed computer-holographic system with a three-color laser is proposed in this Letter. The three-color laser mixed light can calculate the white light suitable for human eyes by a rapid calculation with a modified Gerchberg–Saxton algorithm (MGSA) and an additive color mixing equation drawn up by an International Commission on Illumination (CIE). Parabolic mirrors with distinct curvatures are used for constructing the virtual image projection system to present high-presence 3D images. From the CIE coordinates, it is found that the additive mixed result is within the range of visible light. In this case, primary colors with distinct ratios are additive mixed in order to acquire the appropriate full-color mixed-light ratio. According to color equation in Eq. (1), three color stimuli, blue light ($\lambda = 473$ nm), green light ($\lambda = 532$ nm), and red light ($\lambda = 632$ nm), form white when the mixing is simulated in advance. [W] denotes white light, R, G, and B stand for the mixed ratio of primary colors, and [R], [G], and [B] are the stimulus responses of the cone cells of the human eyes towards the three colors, i.e., the tristimulus values[8]. Matlab is used in this Letter for the white light additive mixing simulation, and the optimal mixed ratio is R:G:B = 3 mW:2 mW:2.6 mW.

$$[\mathrm{W}] = \mathrm{R}[\mathrm{R}] + \mathrm{G}[\mathrm{G}] + \mathrm{B}[\mathrm{B}]. \tag{1}$$

The MGSA is further applied to rapidly calculate the image phase information for generating CGHs[9,10]. It accelerated the speed for image convergence and enhanced the quality of the signal reconstruction in the iterative operation after adding a random phase in the beginning of the algorithm. In addition, the optical structure for the MGSA was a lensless imaging system. A lens can therefore be omitted from the structure in the optical reconstruction in order to simplify the optical structure. Figure 1 shows the flow chart of the MGSA. First, a random phase

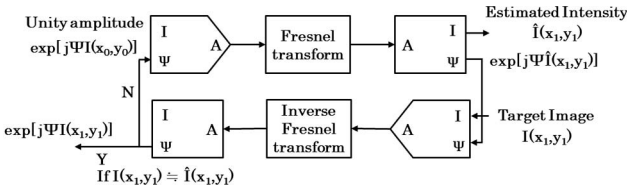

Fig. 1. MGSA processing flowchart.

function is generated, and the initial random phase is denoted as $\Psi I(x_0, y_0)$. Second, the phase function $\Psi\hat{I}(x_0, y_0)$ is multiplied with the initial amplitude for Fresnel transform (FrT), and the approximate image phase function $\hat{I}(x_1, y_1)$ and the approximate phase function $\Psi\hat{I}(x_1, y_1)$ are acquired. Equation (2) is the Fresnel integral transform, where $E(x, y, z)$ is the coordinates of the raw image field, $E(x', y', 0)$ is the coordinates of the raw image plane passing the diffractive image plane of FrT. λ is the wavelength of the incident light, z presents the distance between the hologram and an image plane defined in the space, p is the x-direction spatial frequency, and q is the y-direction spatial frequency.

Third, the target image function $I(x_1, y_1)$ and the approximate image phase function $\Psi\hat{I}(x_1, y_1)$ are proceeded inverse FrT for the phase function $\Psi I(x_0, y_0)$. For the accuracy of an approximate image, the system would repeat steps two and three for image iteration, until the approximate image phase function $\hat{I}(x_1, y_1)$ and the target image function $I(x_1, y_1)$ approach the consistency; the approximate image phase function $\Psi\hat{I}(x_1, y_1)$ is then output. By applying the MGSA to calculate the image phase information, not only is the phase information rapidly acquired, but high-quality image reconstruction can be presented after the decryption.

$$E(x, y, z) = \frac{\exp\frac{j2\pi z}{\lambda}}{j\lambda z}\exp\frac{j\pi}{\lambda z}(x^2 + y^2) \times FrT\{E(x', y', 0) \times \exp\frac{j\pi}{\lambda z}(x'^2 + y'^2)\}$$
$$\text{where } p = \frac{x}{\lambda z}; q = \frac{y}{\lambda z}. \quad (2)$$

After completing the image processing of the computer-generated hologram, a virtual image projection optical architecture is utilized for presenting the full-color stereo image (Fig. 2). The double-parabolic projection system[11,12] is composed of double parabolic mirrors, and the specifications are shown in Table 1. The full-color computer-generated hologram in Fig. 2 is a real image, which could be remade a virtual image through the double-parabolic projection system. The image magnification appears to be 1.2 through the calculation of the paraboloid imaging equation.

Full-color CGHs are applied to the virtual image projection system for experiments using a blue light laser (DPSS Blue LASER, $\lambda = 473$ nm), a green light laser (DPSS Green, $\lambda = 532$ nm), and a red light laser (He–Ne LASER, $\lambda = 632$ nm). The mixed light ratio is R:G:B = 3

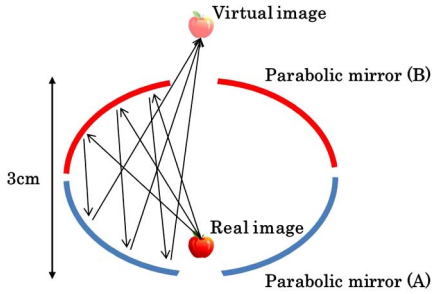

Fig. 2. Architecture of the interactive 3D display system.

Table 1. Specifications of Virtual Image Projection System

	Parabolic Mirror (A)	Parabolic Mirror (B)
Focal Length	50 mm	56 mm
Curvature Radius	100 mm	113 mm
Diameter	140 mm	140 mm
Light Outlet Diameter	40 mm	40 mm

mW:2 mW:2.6 mW, and the system architecture is shown in Fig. 3. When the image phase is calculated through the MGSA, the primary colors' corresponding phase information are input into the SLM for image reconstruction. The pixel pitch of the SLM used in this Letter is 6.4 μm (Jasper Display, Kit JD8554). When the diffractive distance is a fixed value, the reconstructed image is a zero-order diffraction image. The primary color image could be modulated by a 0.6 mm × 1.3 mm white light image through a dichroic prism (X-Cube) (Fig. 4). The white light image could be used to complete the virtual image full-color CGH through the virtual image projection optical architecture (Fig. 5). Figure 5 shows the virtual image projection from a different horizontal angle of view, with which the mixed-light floating image can be

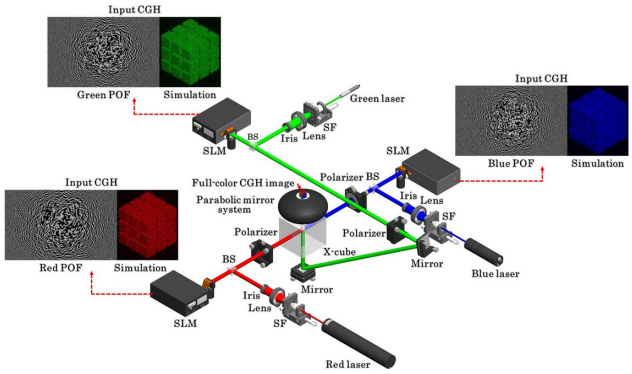

Fig. 3. Application of full-color CGHs to the virtual image projection system.

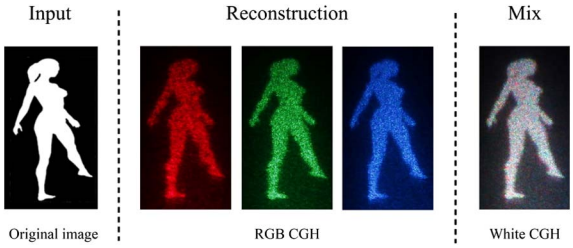

Fig. 4. Virtual image projection of full-color CGHs.

viewed from various angles. The MGSA could merely be applied to the algorithm of two-dimensional (2D) plane patterns in this Letter. The floating images in this Letter are realized through multiple dynamic phase only fuction (POF) and dual parabolic mirrors. The MGSA is utilized to complete several 2D plane-pattern POFs, which are linked and played at a speed of 15 fps, and the dual parabolic mirrors are used for the floating effect. The field of view is generated by the dual-parabolic mirror system, with which the viewers need to view the images at the imaging end of the dual-parabolic mirrors so as to view the 360° perspective from the horizontal viewing angle. In regard to the image quality evaluation, the root mean square error of 0.0524[13] of the CGH imaging can be calculated with Eq. (3), where MN is the reconstruction area, containing the image reconstruction and noise, and I_N is the noise intensity. The relative diffraction efficiency of 95.3% can be calculated with Eq. (4), where I_S is the reconstruction intensity. The horizontal viewing angle is 360°, and the vertical viewing angle ranges from 15° to 75°. As shown in Fig. 6, the color coordinates (x, y) of the full-color mixed image are (0.33,0.39).

$$\text{Root mean square error} = \sqrt{\frac{\sum I_N^2}{MN}}, \tag{3}$$

$$\text{Relative diffraction efficiency} = \frac{\sum I_S}{\left(\sum I_S + \sum I_N\right)}. \tag{4}$$

Fig. 5. Full-color CGH image viewed from distinct horizontal angle of view.

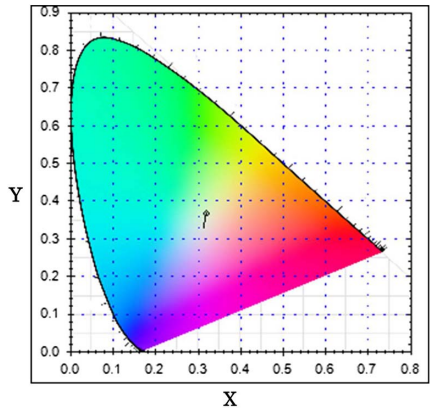

Fig. 6. Color coordinate analysis of white-light CGH image reconstruction.

A full-color projection system with a wide angle of view is implemented in the proposed system. The destruction of spatial coherence and time coherence to restrain the laser speckles is also discussed.

In regard to the destruction of the laser's spatial coherence, the randomly distributed diffuser surface is used to destruct the wavefront and the coherence of the laser light. The destruction degree is determined by the diffuser's roughness. Greater roughness results in the fiercer destruction of the laser light wavefront and coherence[14]. The diffuser diameter is 50.4 mm, and the surface roughness is 0.857 μm. The effect of laser speckle on the images is defined by the laser speckle contrast (SC), which can be obtained using Eq. (5), where I denotes the luminous intensity, ranging from 0–1, and the larger value stands for a more serious laser speckle[15].

$$\text{Speckle contrast} = \frac{\sqrt{\langle I^2\rangle - \langle I\rangle^2}}{\langle I\rangle}. \tag{5}$$

When a diffuser is used for CGH image reconstruction, the SCs of the red light image, green light image, and blue light image are 13.03%, 21.42%, and 26.81%, respectively. When the primary color image reconstruction is modulated as a full-color image reconstruction, the speckle field in the superposition will reduce the laser SC by the nonlinear superposition because the laser speckle pattern in the primary color image reconstruction is mutually superposed[16,17]. In this case, the full-color image reconstruction through mixed light has a SC of 11.75%.

Regarding the destruction of the laser light time coherence, the interference in the middle of an image is more serious than it is at the edge of the image, as a diffuser would have the passing beam generate various optical path differences[18]. For this reason, the diffuser is rotated in this Letter to restrain the interference of the dynamic speckles so that the speckle in the middle or on the edge is homogenized to match the speckle field through dynamic rotation[19]. In addition to pure rotation, the changes of the laser speckle under seven different rotating speeds are further studied and compared (Fig. 7). Under

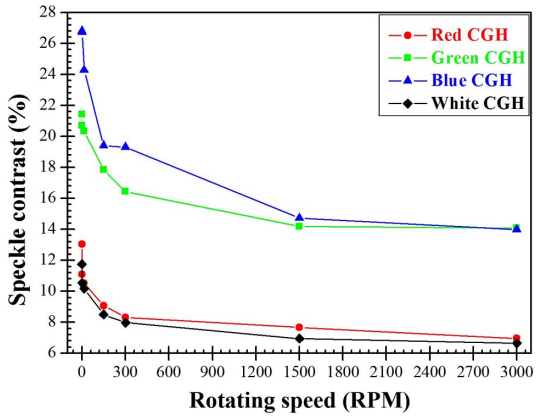

Fig. 7. Changes of laser speckle of red light, green light, blue light, and full-color mixed light image reconstruction under distinct rotating speeds (0, 1.5, 15, 150, 300, 1500, and 3000 rpm).

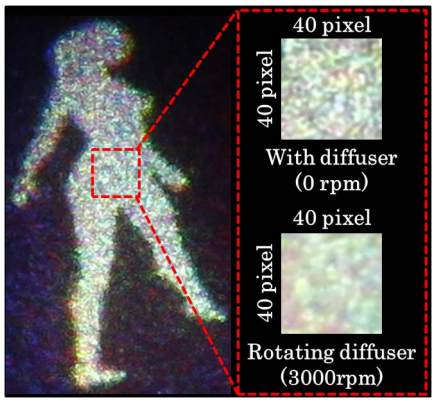

Fig. 8. Image of rotating diffuser with 0 and 3000 rpm retrieved by the CCD.

the revolution of 3000 rpm, the SC of the red light image reconstruction, green light image reconstruction, blue light image reconstruction, and full-color mixed-light image reconstruction drops down to 6.96%, 14.07%, 13.98%, and 6.65%, respectively. Figure 8 shows a 40 pixel × 40 pixel speckle graph retrieved by a CCD without rotation and with the revolution under 3000 rpm. From Fig. 7, it can be seen that the increasing rotation speed would result in the homogeneous distribution of the speckle field and a lower SC. However, when the homogenization is saturated, the restraint becomes stable, even though the revolution is homogenized and the saturated speckle field does not change[20]. In regard to the image speckle restraint, the SC of the full-color computer-generated hologram projected by the system is lower than that proposed by Thomas and Middlebrook[21].

In conclusion, a primary color laser light is used to reconstruct a full-color CGH, and a double-parabolic projection system is utilized for successful image reconstruction, which is presented with a virtual image with high presence. Moreover, restraining the full-color holographic image speckle is also a research point. Meanwhile, the destruction of spatial coherence and time coherence to restrain laser speckle has reduced the mixed-light image speckle down to 6.65%.

This work was supported by the National Science Council of Taiwan, China under contract NSC 101-2628-E-224-002-MY3.

References

1. D. Gabor, Nature **161**, 777 (1948).
2. N. Hashimoto, S. Morokawa, and K. Kitamura, Proc. SPIE **1461**, 291 (1991).
3. Y. Takaki and N. Okada, Appl. Opt. **48**, 3255 (2009).
4. Y. Ohsawa, K. Yamaguchi, T. Ichikawa, and Y. Sakamoto, Appl. Opt. **52**, A167 (2013).
5. X. Xiao, B. Javidi, M. Martinez-Corral, and A. Stern, Appl. Opt. **52**, 546 (2013).
6. B. R. Brown and A. W. Lohmann, IBM J. Res. Dev. **13**, 160 (1969).
7. F. Yaraş, H. Kang, and L. Onural, Appl. Opt. **48**, H48 (2009).
8. W. K. Pratt, *Introduction to Digital Image Processing* (John Wiley & Sons, 2001).
9. H.-E. Hwang, H. T. Chang, and W.-N. Lie, Opt. Express **17**, 13700 (2009).
10. G. Z. Yang, B. Z. Dong, B. Y. Gu, J. Y. Zhuang, and O. K. Ersoy, Appl. Opt. **33**, 2 (1994).
11. H. C. Krah and M. Yousefpor, "Interactive Three-Dimensional Display System," United States patent 0111479A1 (2014).
12. T. Kakue, A. Yoshida, T. Kawashima, K. Suzuki, T. Nishitsuji, T. Shimobaba, and T. Ito, in *Digital Holography and Three-Dimensional Imaging* (Optical Society of America, 2015).
13. J. P. Liu, W. Y. Hsieh, T. C. Poon, and P. Tsang, App. Opt. **50**, H128 (2011).
14. H. Funamizu and J. Uozumi, Opt. Express **15**, 7415 (2007).
15. E. G. Rawson, A. B. Nafarrate, R. E. Norton, and J. W. Goodman, J. Opt. Soc. Am. **66**, 1290 (1976).
16. Q. L. Deng, B. S. Lin, P. J. Wu, K. Y. Chiu, P. L. Fan, and C. Y. Chen, Opt. Express **21**, 31062 (2013).
17. S. V. Egge, M. N. Akram, V. Kartashov, K. Welde, Z. Tong, U. Österberg, and A. Aksnes, Opt. Eng. **50**, 083202 (2011).
18. S. Roelandt, Y. Meuret, G. Craggs, G. Verschaffelt, P. Janssens, and H. Thienpont, Opt. Express **20**, 8770 (2012).
19. C. Y. Chen, Q. L. Deng, P. J. Wu, B. S. Lin, H. T. Chang, H. E. Hwang, and G. S. Huang, Appl. Opt. **53**, G163 (2014).
20. C. Y. Chen, W. C. Su, C. H. Lin, M. D. Ke, Q. L. Deng, and K. Y. Chiu, Opt. Rev. **19**, 440 (2012).
21. W. Thomas and C. Middlebrook, J. Europ. Opt. Soc. Rap. Public. **9**, 14059 (2014).